

A TEST PROGRAM TO EVALUATE THE IMMUNITY OF HS702 SOLAR ARRAY TO SUSTAINED DISCHARGES

P. Leung, C. Gelderloos, J. M. Bodeau, L. Goldhammer, S. Seki and A. Mason
Hughes Space & Communications Company, El Segundo, CA

Abstract

Test results demonstrating the immunity of HS702 100 V array to sustained discharge are presented. For solar array coupon fabricated to HS702 specifications, no sustained discharge was observed even when the potential difference between solar cell strings on the coupon was as high as 200 V. The robustness of the HS702 design is due to the presence of RTV grouting between the solar cells which minimizes the current flow between the edges of the solar cells. Tests to quantify the decay of absolute charging and differential charging during eclipse exit were also performed. Based on the test data, it can be concluded that all potentials on the HS 702 solar array will decay within 20 seconds after the array is exposed to UV with intensity ≥ 0.3 sun.

1. Introduction

The recent partial failures of two solar arrays^{1,2} (not HSC satellites) has reawakened concerns that solar arrays may be vulnerable to electrostatic discharge (ESD)-induced failures, especially the new generations of solar arrays operating at voltages higher than 50 volts. Based on the long record (1000 years of cumulative flight history) of success of its HS376 and HS601 product lines, Hughes Space and Communications Company (HSC) justifiably felt its existing solar array designs were adequately protected. Hughes was preparing to deliver its new 100 Volt dual-junction GaAs HS702 array. Since this is a new design and the array operates at a voltage higher than the operation voltage (≤ 50 Volt) of the previous arrays, HSC began a comprehensive test program to demonstrate the array's immunity to ESD-induced failure. In this report, the test methodologies together with the test results are presented. The results obtained in this test program demonstrate the unique features of HSC's solar array design for the prevention of ESD-induced failures.

Based on published literature¹⁻³, the mechanism proposed to explain the observed on-orbit anomalies requires four separate steps:

- (1) An inverted potential gradient > 500 Volt must develop between coverglass and spacecraft chassis. That is, the coverglass must be charged to a positive potential with respect to the spacecraft structure (including the solar cell). With this potential profile, enhanced electron emission occurs at the triple point junction formed at the vacuum, dielectric and metallic interfaces³ and may lead to discharges.

- (2) An ESD event, or trigger arc, between the coverglass and solar cell or substrate must occur. The ESD event generates a high-density plasma at the discharge site.
- (3) A current flow between the high and low voltage side of a solar cell circuit (which is at a potential difference higher than the threshold voltage) must be sustained for a time period of the order of ms.
- (4) Pyrolyzation of materials between solar cells or between a solar cell and the solar array substrate must occur. Subsequent quenching of the sustained arc leaves a low resistance path; the solar array is then permanently short circuited and unable to deliver power to the spacecraft.

2. Test Methodologies

The approach of this test program is to duplicate the on-orbit charging and discharging phenomena. As mentioned above, the most important feature of solar array charging in sunlight is the inverted gradient potential profile. Therefore, the tests were designed to duplicate this potential profile in the laboratory.

There are two methods to produce the inverted gradient profile. The first method is to use high voltage bias⁴⁻⁶, the second method is to use electron beam and UV irradiation. In this program, both methods are employed.

Since it is difficult to find a facility that allows the use of an entire solar array as a test article, small flight-like coupons were fabricated for this test. A typical coupon consists of two strings of solar cell with a circuit in each string (Figure 1). The coupons

were fabricated to the flight specifications. The flight-like coupons have RTV grouting at the edges of the solar cells. Kapton is used as the substrate insulation material. In addition to the flight-like coupons, control coupons were also fabricated. In the control coupons, the grouting between the solar edge was removed.

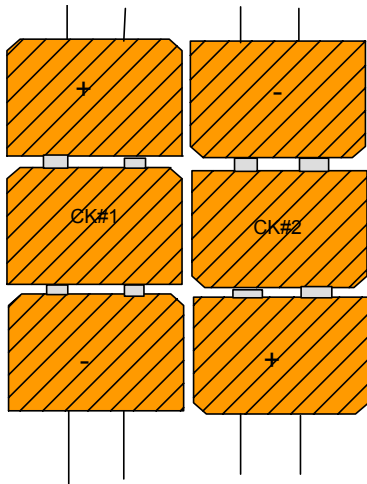


Figure 1. Schematics of the test coupon

It is well known that the energy, charge and current associated with an ESD event scale with the area. In this test program, the tests were performed with a small coupon. As compared to a spacecraft with large solar panels, a small coupon has a lower capacitance with respect to ground and hence lower stored charge and energy. Since the density of ESD-produced plasma is proportional to charge released, the discharge event produced by a small coupon cannot provide the same plasma conditions as a solar panel discharge. In order to compensate for the low capacitance value of a small coupon, an external capacitance is added to the small coupon. The value of capacitors used in this program ranges from 0.007 μF to 0.15 μF .

3. High Voltage Bias Test

The setup for the high voltage bias test is shown in Figure 2. The coupon is mounted on top of a temperature control plate. It is isolated from the chamber ground by a piece of Teflon. Figure 3 shows the circuit diagram for biasing the coupon. A solar array simulator (SAS) is used to apply a potential difference between the two strings of the solar array coupon. SAS is essentially a power supply, but it has lower capacitance than a regular power supply. The voltage and current (steady state) outputs of SAS are adjustable. The low side of the SAS is connected to the chassis (structure) of the test

coupon. A high voltage power supply is used to bias the coupon structure to a negative high voltage with respect to ground, simulating the charging of spacecraft structure in space. A limiting resistor (1 M Ω to 10 M Ω) is used to isolate the power supply from a discharge event. Current probes are used to monitor the currents generated during a discharge event. The locations of these current probes are shown in Figure 3.

An electron beam produced by an electron gun is used to illuminate the front surface of the solar array coupon. Usually, the energy of the beam is chosen such that the electrons arriving at the coupon have an energy of 300 eV. For CMG coverglass material, the secondary electron yield at this energy is > 1 . The resulting secondary electron emission causes the coverglass to be charged to a positive potential with respect to structure. The coverglass potential is measured by a non-contacting voltmeter, which is manufactured by Trek (Trek Probe).

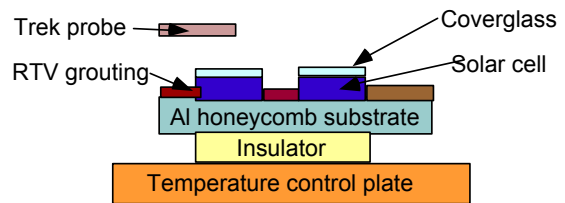
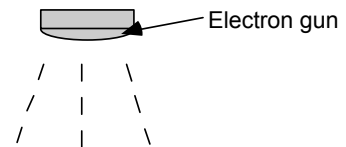


Figure 2. Setup for high voltage bias test

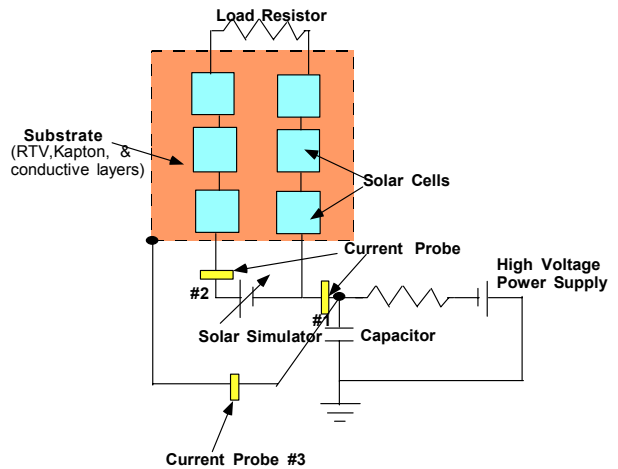


Figure 3. Schematics of bias circuitry

Tests were performed in a vacuum chamber with a base pressure less than 4×10^{-6} torr. Most of the tests were performed with the solar array coupon structure/chassis biased at 2 KV. At this bias voltage, the energy of the incident electron beam was set at 2.3 KeV. The current density of the electron beam was 0.5 nA/cm^2 . This current density simulates the worst case electron current in GEO environment. Tests were performed with the solar array coupon at temperatures ranging from $-10 \text{ }^\circ\text{C}$ to $140 \text{ }^\circ\text{C}$. The upper temperature limit represents the highest possible operation temperature of the HS702 array. Capacitors with values of $0.03 \text{ }\mu\text{F}$ and $0.1 \text{ }\mu\text{F}$ were used as the external capacitors (C_{ext}). The bias between the solar cells strings was varied between 0 to 200 Volt. The upper voltage limit is twice the operation voltage of the HS702 array. The current output of SAS was either set to 0.7 Amp or 1.4 Amp. The latter value is twice the current available in each string of the HS702 solar array.

A differential voltage (δv) between the coverglass and solar cell/structure developed when the coverglass was irradiated by electron beam. The magnitude of differential charging was observed to decrease with an increase in temperature. At $140 \text{ }^\circ\text{C}$, the potential difference between the coverglass and structure was less than 100 V. Two HS702 coupons were used for this test. Table 1 displays the maximum differential charging as a function of temperature for these two coupons. For both coupons, δv decreased with an increase in temperature. This charging characteristic agrees with the observed temperature dependence of the resistivities of the insulating materials (coverglass, RTV, and adhesive) on the solar array. The resistivities of these materials were observed to decrease with an increase in temperature.

Table 1. Summary of high voltage bias test

Temp. ($^\circ\text{C}$)	HS702 #1		HS702 #2	
	δv (V)	ESD	δv (V)	ESD
-12	1360	Yes	1350	Yes
18	1170	Yes	1400	Yes
70	830	No	880	Yes
140	240	No	500	No

Discharges started to occur when the magnitude of differential charging $\geq 880\text{V}$. In most of the discharge events, the energy stored in the capacitor was depleted during a discharge event as evidence by the fact that the voltage on the capacitor decreased to zero after a discharge event.

A voltage bias was applied across the strings, and the current flow between the strings was monitored (string current). The observed string current characteristics can be divided into three categories. They are: (1) no coupling, (2) coupling, and (3) sustained discharge.

No coupling implies that the string current extinguishes immediately after a discharge. Figure 4 shows an example of no coupling. The peak current of the main discharge pulse was $\sim 40 \text{ A}$ (measured by current probe#3). During this main discharge pulse, there was a small current (peak current $\sim 4 \text{ A}$) flowing between the solar cell strings. However, this string current extinguished immediately when the discharge current decreased to zero.

Coupling means that there is a significant follow-on current even after the main trigger discharge is extinguished. Figure 5 shows the waveform of a discharge event showing coupling between the solar cell strings. A current pulse with a peak current of 2 Amp and a width of $2 \text{ }\mu\text{s}$ was observed after the main discharge was over. For this event, the total charge released in this follow-on current pulse is less than 1% of the charge stored in the solar simulator. With the HS702 coupon, the threshold voltage for coupling was observed to be $\sim 150 \text{ V}$.

A sustained discharge occurs when there is a long duration current pulse after the initial trigger arc. In a sustained discharge, the charge stored in SAS is depleted by this follow-on current pulse. With the regular HS702 coupons, a sustained discharge was not observed at a voltage bias of 200 volts and even with an external capacitor as high as $0.1 \text{ }\mu\text{F}$.

Tests were also performed with the control coupon. The control coupon does not have grouting in between the cells. The results obtained with the control coupon were very revealing. Coupling between the solar cell strings occurred at 70 V, much lower than the 150 V that was required for a regular coupon. At a bias of 110 V, a sustained discharge occurred. Figure 6 shows the waveform of a sustained discharge event. The entire waveform was not captured. However, video image of this event indicated that this ESD event lasted 4 standard frames (30 frame per second). Consequently, the time duration of this event was at least 120 ms. After this event was over, the SAS went into current limited mode, and was supplying a steady state current of 0.7 Amp. Further examination indicated that the Kapton insulation in the substrate had been pyrolyzed causing a short between solar cells.

4. UV and Electron Beam Irradiation Test

For this test, the solar array coupon is mounted on guarded isolated ceramic standoffs (Figure 7). The standoffs enable the solar array structure to be electrically isolated from the chamber ground. The charging of the solar array is achieved by irradiating the backside of the array with an electron beam. The structure (chassis) potential is obtained by measuring the potential of the back surface with a high impedance ($10^{13} \Omega$) resistor divider network. With this high impedance, the array will not be shorted to ground by the current flowing through this resistor network, thus keeping the solar cell coupon floating electrically.

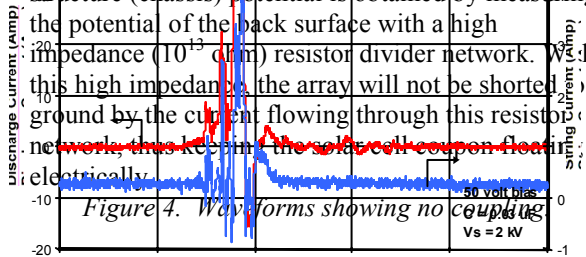
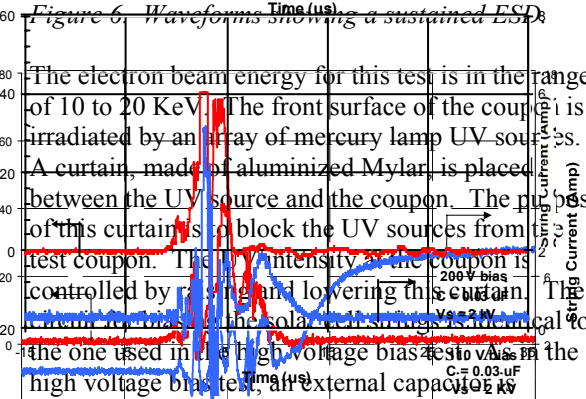


Figure 5. Waveforms showing coupling.

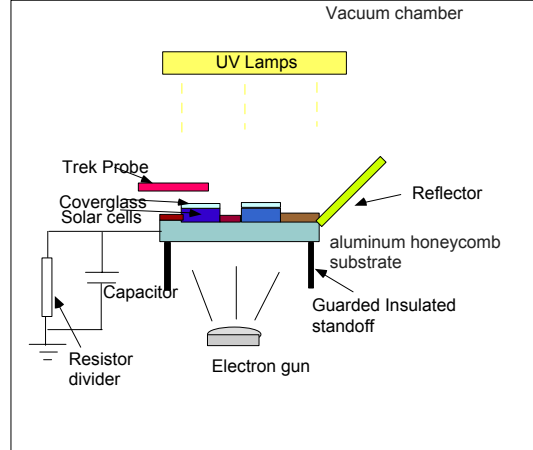


The electron beam energy for this test is in the range of 10 to 20 KeV. The front surface of the coupon is irradiated by an array of mercury lamp UV sources. A curtain, made of aluminized Mylar, is placed between the UV source and the coupon. The purpose of this curtain is to block the UV sources from the test coupon. The UV intensity at the coupon is controlled by raising and lowering this curtain. The current ratios of the solar cell strings is identical to the one used in the high voltage bias test. An external capacitor is installed between the solar array structure ground and chamber ground. Two different external capacitors

were used for this test, their values were $0.007 \mu\text{F}$ and $0.03 \mu\text{F}$. The coverglass potential is measured by Trek probe. In some of the tests, a 15 cm by 15 cm aluminum sheet was installed at the front surface of the coupon (Figure 7). This sheet simulates the reflector on the HS702 array. NASCAP analysis⁸ has indicated that under sunlit condition, no charging is possible when reflectors are present. This prediction was indeed verified by these tests. Therefore, this reflector was only used for tests to study the decay of surface potentials in penumbra. This reflector was removed in tests performed to characterize the discharge parameters.

In the absence of UV, the backside of the coupon was charged to a negative potential by electron beam irradiation. In general, the structure voltage was 2-4 KV below the beam energy. That is, when the beam energy was 10 KeV, the structure was charged to a voltage of -6 to -8 KV. When the UV source was turned on, photoelectron emission caused the coverglass to achieve a positive potential, (i.e. less negative) with respect to the structure. Discharges were observed under these conditions. The magnitude of differential charging required for a discharge to occur was in the range of 1 to 4 KV. The characteristics of the discharge current waveform were similar to the waveforms obtained in the high voltage bias test.

Figure 7. UV-electron beam irradiation test setup



As in the high voltage bias test, the coupling between the strings increased as the bias between the strings was raised. At a bias voltage of 150 V, significant coupling between the strings was observed. However, no sustained discharge was ever observed with the HS702 coupon, even when the bias voltage was increased to 200 V.

Tests were also performed with a control coupon (control coupon#2). This control coupon exhibited efficient coupling even when the potential difference between the solar cell strings was below 50 V. A sustained discharge occurred when the bias across strings of the control coupon was only 50 V. For this event, the observed peak current was approximately 40 Amp. The duration of the sustained current was 100 μ s. The discharge was quenched because the charge stored in SAS was depleted by the sustained current pulse. When the discharge was over, SAS went into the current limited mode (limited to 0.7 Amp for this run). Resistance measurements showed that a short had developed between the edge of solar cells.

5. Decay of Surface Potentials in Penumbra

The goal of this test is to determine the time required for the decay of absolute potential and differential potential during eclipse exit. The test setup is shown in Figure 7 (with the reflector installed). The area of the reflector is approximately equal to the total area of coverglass.

In a typical test, an electron beam was used to irradiate the backside (structure) of the coupon, causing the structure to charge to a negative potential. At the beginning of each test, the UV sources were turned on. The coupon was blocked from UV light by the aluminized Mylar curtain. The aluminized Mylar curtain was then manually lowered to a predetermined location corresponding to a specific UV intensity. This simulates the transition from eclipse to penumbra. The electron beam was on all the time, simulating the condition in which the substorm electron environment is present during eclipse and during eclipse exit. For most tests, the electron beam parameters were set to simulate the 90% substorm environment specified in NASA Spacecraft Charging Design Guidelines⁷, that is, 12 KeV at a current density 0.5 nA/cm².

As predicted by NASCAP analysis⁸, whenever the coupon was exposed to UV, the structure potential decayed rapidly. Figure 8 shows a typical potential decay profile when the solar array coupon was exposed to UV intensity of 0.3 sun. The structure

was initially charged by electron beam irradiation to -4 KV. The potential of coverglass was -2 KV, resulting in a differential charging level of 2 KV. When the curtain was lowered (several seconds were required to lower the curtain to the right position) and the coupon was exposed to UV, both the structure potential and the coverglass potential dropped rapidly. The differential charging level remained at 2 KV for approximately one second. The coverglass potential reached ground potential first and then overshot to \sim +50 volt. At this time, the structural potential dropped to -500 V and the potential decay stopped momentarily. The explanation for this behavior is that the space charge of the photoelectrons emitted by coverglass and the aluminum reflector formed a negative potential well in the vicinity of the coupon causing the photoelectrons to return to the coupon. The negative potential well decayed when the emitted photoelectrons eventually diffused to chamber wall. At this time, photoelectrons emitted by the coupon could escape the coupon again. The phenomenon of photoelectrons returning to their emitting source has also been observed on SCATHA spacecraft⁹.

Figure 9 shows another potential decay profile. For this test, the coupon was exposed to UV with intensity corresponding to 0.5 sun. The initial rate of decay of the surface potentials was faster than the previous case. The potential decay also stopped momentarily (after \sim 5 seconds of exposure to UV) due to space charge effect. The coverglass and structure potentials eventually reached ground potential. The total time for the decay of absolute and differential potentials was approximately 10 seconds after exposure to UV.

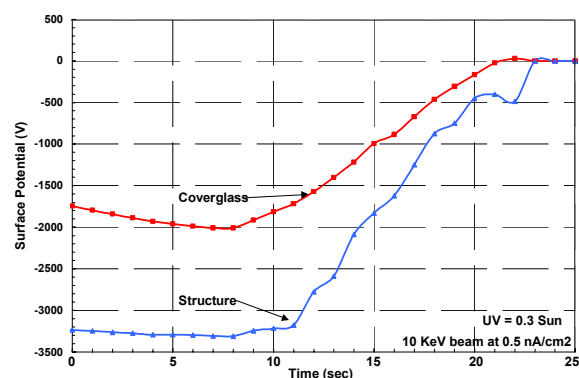


Figure 8. Surface potential decay with the UV intensity at 0.3 sun.

Tests were performed with varying initial conditions, and with UV intensities in the range of 0.3 to 2 suns.

In all these tests, the decay time for the absolute and differential charging was less than 20 seconds.

At a sun intensity of 0.3 sun, the solar array has not built up to full voltage/power. Even if a trigger ESD event occurs during penumbra, there is not sufficient voltage/power from the HS702 S/C solar array to feed a sustained discharge event. Consequently, a sustained discharge is unlikely to occur during penumbra.

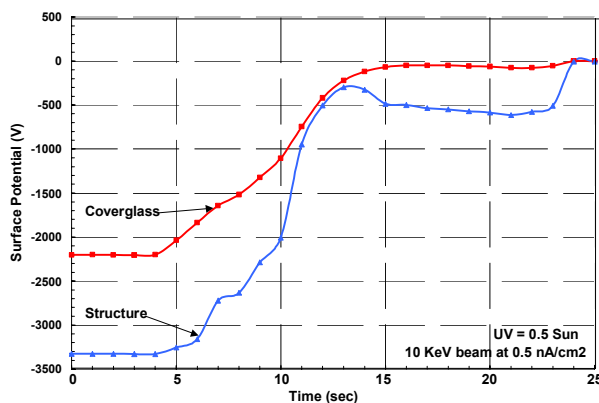


Figure 9. Surface potential decay with the UV intensity at 0.5 sun.

6. Conclusions

This test program has demonstrated the robustness of the HS702 100 V solar array. It is not susceptible to sustained discharge. Based on the test results, the threshold voltage for a sustained discharge to occur is > 200 V, giving a voltage margin of > 2 . In addition, the current output capability of SAS during the test was as high as 1.4 A which is twice the current output of each solar cell string, giving a current margin of 2.

The main design feature that is responsible for the robustness of this array is the RTV grouting between the solar cells. This grouting provides a barrier between the ESD produced plasma and the solar cells, and minimizes the current flow between the cells.

Due to the presence of large sunlit conducting solar reflectors, NASCAP analysis⁸ has indicated that HS702 will not be subjected to absolute and differential charging in sunlit conditions. In eclipse, absolute and differential charging are possible. However, test results presented in this paper show that the potentials resulting from absolute and differential charging will decay completely before the

voltage/power on the solar array are fully developed, further minimizing the probability of occurrence of a sustained discharge.

The test results also show that at the operation temperature of HS702 solar array, it cannot achieve a differential charging level that is adequate for a trigger arc to occur. Consequently, the dense plasma that is needed for a sustained discharge to occur will be absent in flight condition. In conclusion, the HS702 100 V solar arrays will not be susceptible to sustained discharges and therefore no irreversible electrical degradation of the solar arrays will occur on-orbit.

7. References

1. Katz, Davis, and Snyder, "Mechanism for Spacecraft Charging Initiated Destruction of Solar Arrays in GEO," AIAA 36th Aerospace Sciences Meeting, Reno, Nevada, 1998.
2. Hoerber, et al., "Solar Array Augmented Electrostatic Discharge In GEO," AIAA Yokohama Conference, 1998.
3. M. Cho and D. E. Hastings "Computer Particle Simulation of High-Voltage Solar Array Arcing Onset," Journal of Spacecraft and Rockets, Vol. 30, No. 2, Mar./Apr. 1993, pp. 190-201.
4. Stevens, et al., "Voltage Gradients in Solar Array Cavities as Possible Breakdown Sites in S/C Charging Induced Discharges," IEEE Transactions on Nuclear Science, Vol. NS-28, No. 6, Dec. 1981, pp. 4558-4562.
5. D. Snyder, "Environmentally Induced Discharges in a Solar Array," IEEE Transactions on Nuclear Science, Vol. NS-29, No. 6, Dec. 1982, pp. 1607-1609.
6. P. Leung, "Discharge Characteristics of a Simulated Solar Cell Array," IEEE Transactions on Nuclear Science, Vol. NS-30, No. 6, Dec. 1983, pp. 4311-4315.
7. C. Purvis, H. Garrett, A. Whittlesy and N. Stevens, "Design guidelines for Assessing and Controlling Spacecraft Charging Effects", NASA TP 2361 Purvis, H. Garrett, A. Whittlesy and N. Stevens.

8. V. Davis, I. Katz, P. Leung, C. Gelderoos, "Spacecraft Charging Analysis of the Hughes 702 Satellite", submitted for Publication in the Proceedings of 6th Spacecraft Charging Conference.
9. M.S. Gussenhoven and E.G. Mullen, "SCATHA Retrospective: Satellite Frame Charging and Discharging in the Near-Geosynchronous Environment", submitted for Publication in the Proceedings of 6th Spacecraft Charging Conference.